Supplementary Information

Facet-Selective Growth on Nanowires Yields Multi-Component Nanostructures and Photonic Devices

Thomas J. Kempa,[†] Sun-Kyung Kim,[†,◊] Robert W. Day,[†] Hong-Gyu Park,[*§] Daniel G. Nocera,[*†] and Charles M. Lieber[*†,‡]

[†]Department of Chemistry and Chemical Biology and [‡]School of Engineering and Applied Sciences, Harvard University, Cambridge, Massachusetts 02138. [◊]Department of Applied Physics, Kyung Hee University, Gyeonggi-do, Republic of Korea. [§]Department of Physics, Korea University, Seoul 136-701, Republic of Korea.

email: cml@cmliris.harvard.edu

Index		*Page*
Materials and Methods		S2–S5
Fig. S1	Role of template surface for facet selective growth of Ge	S6
Fig. S2	Facet selective Si homoepitaxial growth	S7
Fig. S3	TEM cross-section preparation and images	S8
Fig. S4	EDS spectrum of nanostructure with embedded Ge regions	S9
Fig. S5	TEM of Si/Ge/Si interface near {011}	S10
Fig. S6	EQE spectra of NW devices containing nanocavities	S11

Materials and Methods

Nanowire Syntheses

Si Nanowire (NW) Template. Au catalysts (100 nm diameter) were dispersed on poly-L-lysine functionalized 600 nm SiO_2-on-Si wafers. Substrates were inserted into a home-built quartz-tube reactor and the system was evacuated to 2.8 mTorr base pressure. Crystalline intrinsic Si nanowire (NW) cores were grown at 460 ˚C and 40 Torr for 1 h with flow rates of 1 and 60 standard cubic centimeters per minute (sccm) for silane (SiH_4), and hydrogen (H_2, Semiconductor Grade), respectively. A crystalline intrinsic Si shell was grown over these cores at 775 ˚C and 25 Torr for 30 min with flow rates of 0.15 and 60 sccm for silane and hydrogen, respectively.[1] A calibrated shell growth rate of 1.7 nm/min was determined from independent studies of shell thickness vs. growth time.

*Structure **1**.* Immediately following synthesis of the **Si NW template**, the reactor was purged to base pressure and re-pressurized to 4 Torr with a hydrogen flow rate of 20 sccm. This step was completed within 10 s. While pressurized, the reactor was cooled from 775 ˚C to 200 ˚C over 15 min. Once the reactor cooled to be sure that the sample was below the final Ge growth temperature, the furnace lid was closed and its heater turned back on. The Ge growth temperature set point (330˚C) was reached within 3 min. Facet selective synthesis of Ge was carried out at 330˚C and 5.8 Torr for 5 min with flow rates of 10 and 20 sccm for germane (GeH_4, 10% in H_2) and hydrogen, respectively.

*Structure **2**.* Immediately following synthesis of the **Si NW template**, the reactor was purged to base pressure and argon (Ar, Semiconductor Grade) introduced at a flow rate of 20 sccm. With argon continuously flowing, the reactor was cooled from 775 ˚C to 300 ˚C over 5 min. Once the reactor cooled to be sure that the sample was below the final Ge growth temperature, the furnace lid was closed and its heater turned back on. The Ge growth temperature set point (380˚C) was reached within 3 min. Facet selective synthesis of Ge was carried out at 380 ˚C and 10 Torr for 5 min with flow rates of 10, 10, and 20 sccm for germane, phosphine (PH_3, 1000 ppm in H_2) and argon, respectively.

*Structure **3**.* Immediately following synthesis of the **Si NW template**, the reactor was purged to base pressure and cooled under vacuum from 775 ˚C to 300 ˚C over 5 min. Once the reactor cooled to be sure that the sample was below the final Ge growth temperature, the furnace lid was closed and its heater turned back on. The Ge growth temperature set point (380˚C) was reached within 3 min. Synthesis of a conformal Ge shell was carried out at 380 ˚C and 4 Torr for 5 min with a flow rate of 5 sccm for germane.

Structure in Fig. 3. Crystalline *p*-type Si NW cores were grown at 460 ˚C and 40 Torr for 1 h with flow rates of 1, 5 and 60 sccm for silane, diborane (100 ppm in H_2) and hydrogen,

[1] Kempa, T. J.; Cahoon, J. F.; Kim, S-K.; Day, R. W.; Bell, D. C.; Park, H-G.; Lieber, C. M. *Proc. Natl. Acad. Sci. USA* **2012**, *109*, 1407–1412.

respectively. A crystalline *p*-type Si shell was grown over these cores at 775 ˚C and 25 Torr for 5 min with flow rates of 0.15, 1.5 and 60 sccm for silane, diborane and hydrogen, respectively. Next a crystalline intrinsic Si shell was grown over these cores at 775 ˚C and 25 Torr for 15 min with flow rates of 0.15 and 60 sccm for silane and hydrogen, respectively. Immediately following this synthesis, the reactor was purged to base pressure and re-pressurized to 4 Torr with a hydrogen flow rate of 20 sccm. While pressurized, the reactor was cooled from 775 ˚C to 200 ˚C over 15 min. Once the reactor cooled, the furnace lid was closed and its heater turned back on. The Ge growth temperature set point (330˚C) was reached within 3 min. Facet selective synthesis of Ge was carried out at 330 ˚C and 5.8 Torr for 7 min with flow rates of 10 and 20 sccm for germane and hydrogen, respectively. Next, the reactor was heated under vacuum to 550 ˚C and held at this temperature for 1 min. Synthesis of a conformal shell of *n*-type Si was carried out at 550 ˚C and 5 Torr for 1.5 min with flow rates of 2 and 10 sccm for silane and phosphine.

Structure in Fig. S1. Immediately following synthesis of the **Si NW template**, the reactor was purged to base pressure and cooled under vacuum from 775 ˚C to 400 ˚C over 4 min. Once the reactor cooled, the furnace lid was closed and its heater turned back on. The Si growth temperature set point (450˚C) was reached within 3 min. Synthesis of a conformal amorphous Si layer was carried out at 450 ˚C and 5 Torr for 1 min with a flow rate of 2 sccm for silane. Next, the reactor was purged to base pressure, re-pressurized to 4 Torr with a hydrogen flow rate of 20 sccm, and cooled over 2 min to 200 ˚C. Subsequent synthesis conditions were as for structure **1**.

Structure in Fig. S2. Immediately following synthesis of the **Si NW template**, the reactor was purged to base pressure and hydrogen introduced at a flow rate of 60 sccm. With hydrogen continuously flowing, the reactor was cooled from 775 ˚C to 650 ˚C over 10 min. Facet selective synthesis of Si was carried out at 650 ˚C and 25 Torr for 20 min with flow rates of 0.15 and 60 sccm for silane and hydrogen, respectively.

TEM and EDS Sample Preparation and Characterization

Cross-sections for TEM studies were prepared by embedding NW structures in epoxy (Epo-Tek 353ND, Epoxy Technology). Samples were degassed to remove air bubbles and cured for 12 h at 30 ˚C in a vacuum oven. A diamond knife (Ultra 35˚, DiATOME) was used with a sectioning tool (Ultra Microtome, Leica) to cut ~40 – 60 nm thick sections from the cured epoxy slugs. We note that the embedded nanowires have a distribution of orientation with respect to the growth substrate. During microtoming, this will lead to cross-sections that are cut off the nanowire growth axis, and thus yield a cross-section morphology that can vary from that expected for the ideal perpendicular section (Figure S3). The samples were transferred to lacey carbon grids for TEM analysis (JEOL 2100, JEOL Ltd.). An aberration corrected scanning TEM (cs-STEM, Libra 200 MC, Carl Zeiss NTS) equipped with twin EDS detectors and drift correction was used for acquisition of the EDS elemental map and

spectrum shown in Figs. 3C and S3. These EDS data were acquired at 1024 × 800 resolution over 1 h using a 400 ms pixel dwell time and 1.2 nm spot size with beam energy of 200 kV. An SEM (Supra 55VP, Carl Zeiss NTS) equipped with EDS detector was used for acquisition of the EDS elemental maps shown in Fig. 1C. These EDS data were acquired at 512 × 400 resolution over 20 min using a 500 μs pixel dwell time with beam energy of 4 kV.

NW Nanostructure Device Fabrication

NW nanostructures were synthesized with 10 and 20 nm wide embedded Ge regions (*Structure in Fig. 3.*) and then covered with a 30 nm conformal layer of SiO_2 using plasma enhanced chemical vapor deposition (PECVD). These nanostructures were shear transferred from their growth substrates to Si_3N_4.[2] SU-8 2000.5 was spin-coated to a thickness of 500 nm over the device substrate, pre-baked (95 ˚C), and electron beam lithography (EBL) was used to define SU-8 etch masks over a portion of the nanostructure. SU-8 was developed and cured for 10 min at 180 ˚C. Subsequently, etching to the *p*-type Si core was accomplished in the following order: 5 sec in BHF (for removal of the outer SiO_2 shell), 10 sec in potassium hydroxide (KOH 38 vol.% in water) at 60 ˚C, 10 s in hydrogen peroxide (30 vol.% in water) at 60 ˚C, and 12 sec in potassium hydroxide at 60˚C. To selectively etch Ge from[3] the nanostructure, the device substrate was immersed in hydrogen peroxide at 60 ˚C for 30 min. Lastly, EBL followed by thermal evaporation of 4 nm of Ti and 300 nm of Pd was performed to define ohmic contacts to the etched (*p*-type) core and un-etched (*n*-type) shell. For the demonstration shown in Fig. 4C, a water solution containing 5 nm Au nanoparticles (Ted Pella, Inc.) was dropped onto the surface of an epoxy plug and allowed to evaporate. This plug was previously embedded with the Ge-etched nanowire structures (Fig. 4B) whose ends were exposed at its surface. Longitudinal TEM cross-sections ~100 nm thick were prepared by microtoming this slug at a 70˚ angle.

Device EQE spectra

Polarization-resolved photocurrent spectra were obtained on a home-built optical setup1 utilizing a standard solar simulator (150 W, Newport Oriel) with AM 1.5G filter as illumination source, a spectrometer (SpectraPro 300i, Acton Research) with 1200 g/mm grating and blaze angle of 500 nm, and an uncoated Glan-Thompson calcite polarizer (10GT04, Newport). Illumination power was measured using a power meter and low-power Si photodetector (1918-C and 918D-UV-OD3, Newport). Power spectra were acquired from 300 to 900 nm in 5 nm increments through 1.0, 1.3, and 2.0 mm diameter circular apertures to verify uniformity and accuracy of the power density used to calculate absolute EQE values. Nanostructure device photocurrents for transverse-electric (TE) and

[2] Javey, A.; Nam, S. W.; Friedman, R. S.; Yan, H.; Lieber, C. M. *Nano Lett.* **2007**, *7*, 773−777.

[3] Williams, K. R.; Gupta, K.; Wasilik, M. *J. Microelectromech. S.* **2003**, *12*, 761−778.

transverse-magnetic (TM) polarizations were measured from 300 to 900 nm in 5 nm increments using a semiconductor parameter analyzer (4156C, Agilent Technologies). Absolute EQE spectra were calculated using the wavelength-dependent photocurrent data collected as described above and the projected area of the nanostructures, which was measured by SEM. The projected area of the nanostructure was taken to be the exposed area of the un-etched nanostructure when viewed perpendicular to the substrate plane and did not include the area covered by the 300 nm thick metal contacts.

FDTD calculations

The absorption cross section of the simulated nanostructures under illumination by a normally incident plane wave was obtained by integrating $J \cdot E$ at each grid point, where J and E are the polarization current density and electric field, respectively. The absorption cross section was integrated over one optical period, and the wavelength of incident light was scanned from 280 – 1000 nm in 5 nm increments. The absorption efficiency is the ratio of the nanostructure absorption cross section to its physical cross section. Lastly, EQE is calculated by multiplying the absorption efficiency by internal quantum efficiency (IQE), where IQE was assumed to be unity. The nanostructure was simulated as a volume element with hexagonal cross-section and a spatial resolution of $5/\sqrt{3}$, 5, and 5 nm for x, y and z, respectively, where y lies along the nanostructure axis and z lies along the propagation direction of the incident plane wave. The simulated nanostructures had diameters of 230 nm, with 0, 10, or 20 nm wide air-filled cavities positioned 20 nm from the Si surface. All simulations included the Si_3N_4 device substrate and conformal SiO_2 layer used in the experiment. Periodic boundary conditions were applied along the axis of the nanostructure. To ensure that a single nanostructure experiences an infinite plane wave, we implemented the total-field scattered-field (TFSF) method. Without this method, a single nanostructure would be simulated as a periodic array of nanostructures along the x-axis. The measured refractive index and extinction coefficient of single crystal silicon[4] over the wavelength range, 280 – 1000 nm, was incorporated into the FDTD simulation.

[4] Lide, D. R. *CRC Handbook of Chemistry and Physics: A Ready-reference Book of Chemical and Physical Data*; CRC Press: Boca Raton, 2008.

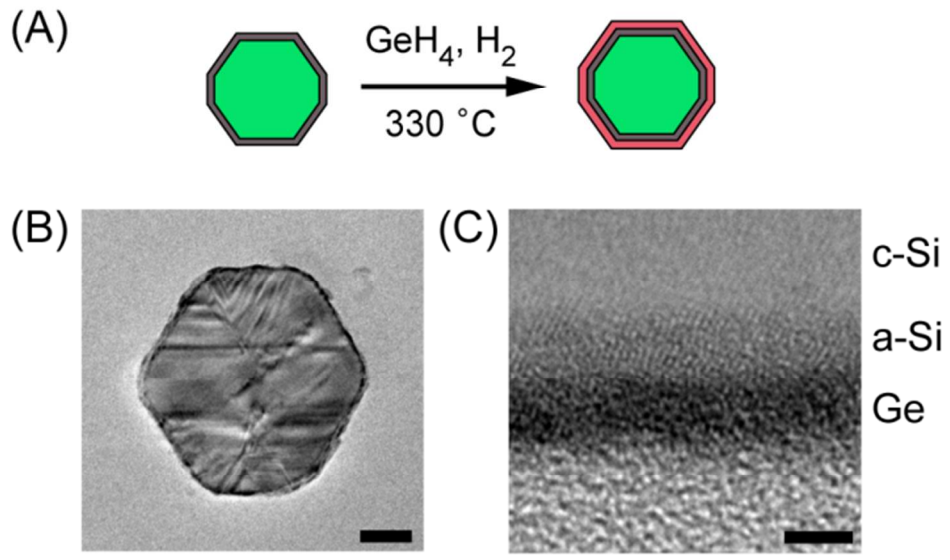

Figure S1. Role of template surface for facet selective growth of Ge. (A) Schematic of synthesis conditions which are identical to those for structure **1**. The Si template (green) has been covered with an amorphous Si shell (gray). (B) Bright-field TEM of a 40 nm thick cross-section of the nanostructure grown as outlined in (A). Image is oriented with {111} surfaces on top and bottom. Scale bar, 50 nm. (C) High-resolution TEM near {111} surface identifying the intentionally deposited amorphous Si shell and a thin conformal Ge shell. Scale bar, 3 nm.

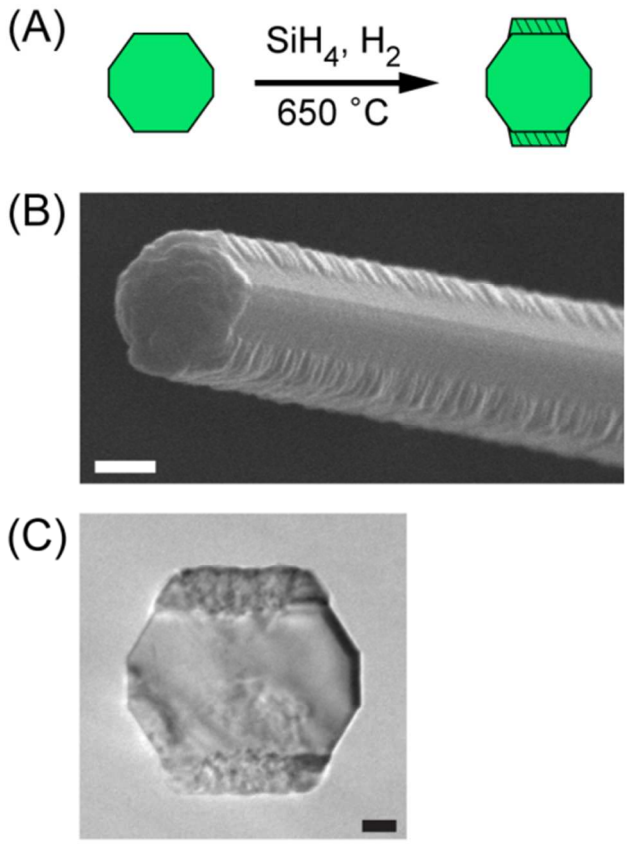

Figure S2. Facet selective Si homoepitaxial growth. (A) Schematic outlining synthesis conditions for facet-selective growth of Si on a Si template (green). (B) SEM of the nanostructure grown as outlined in (A). Image is oriented with {111} surfaces on top and bottom. Scale bar, 200 nm. (C) Bright-field TEM of nanostructure cross-section with {111} surfaces oriented on top and bottom of image. Scale bar, 50 nm. Facet-selective Si deposition is clearly visible on the {111} surfaces. By comparing the dimensions and facet lengths of the nanostructure against these same values for the template we confirmed that no Si grew on the {113} and {011} surfaces.

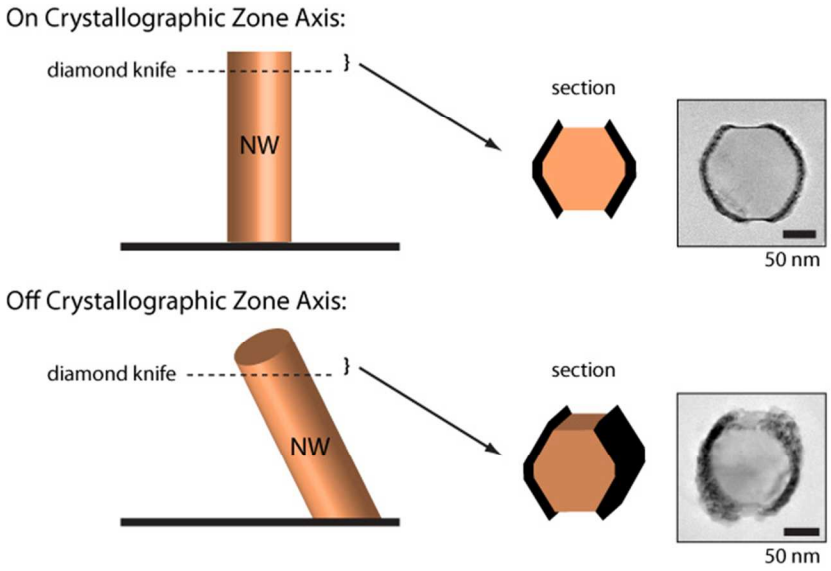

Figure S3. TEM cross-section preparation and images. As grown NWs have a range of orientations with respect to the growth substrate, and the sectioning plane of the diamond knife is parallel to the growth substrate for TEM cross-section sample preparation. In the ideal case, the diamond knife produces a section orthogonal to the NW's growth axis producing an undistorted axial slice when viewed in the TEM. In most cases, the diamond knife intercepts the NW at an angle off the nanowire axis thereby producing a distorted axial slice as observed in many TEM images. The upper and lower TEM images in the figure show ca. undistorted perpendicular and distorted off-axis cases, respectively.

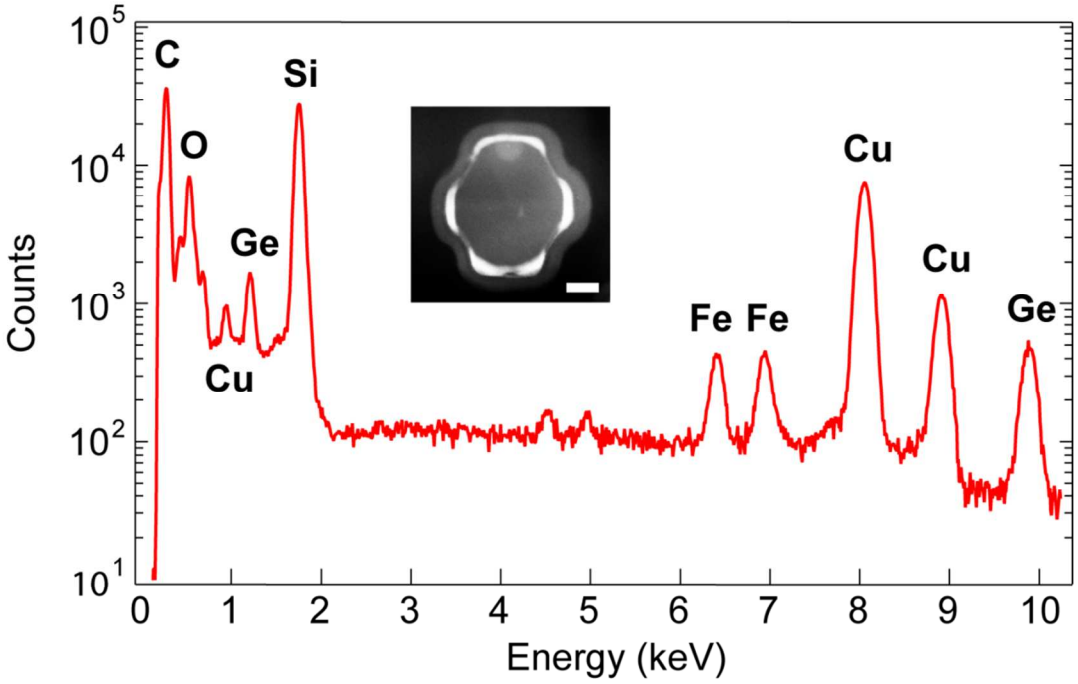

Figure S4. EDS spectrum of nanostructure with embedded Ge regions. EDS spectrum of a 40 nm thick cross-section (inset) of the nanostructure with Ge embedded within Si *p-n* junction. Ge Lβ (1.21 keV), Ge Kα (9.88 keV), and Si Kα (1.76 keV) lines are clearly discernable. Inset: dark-field TEM of the cross-section used to acquire the EDS spectrum. Scale bar, 50 nm.

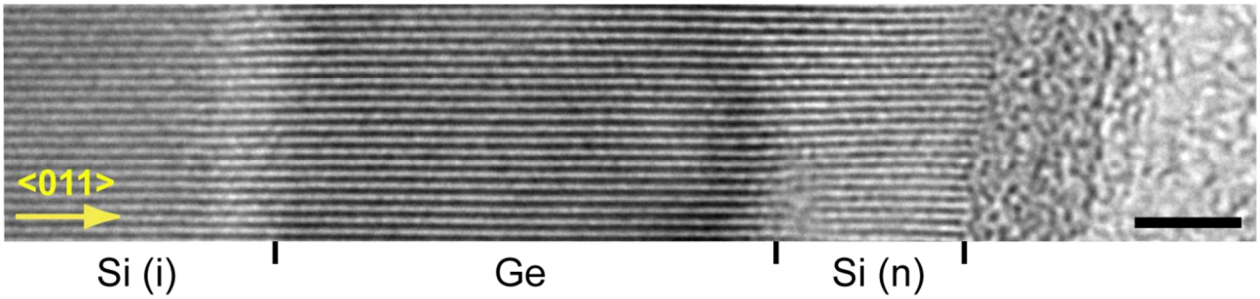

Figure S5. TEM of Si/Ge/Si interface near {011}. High-resolution TEM of the intrinsic Si/Ge/*n*-Si region near the {011} interface within the nanostructure. The {011} plane lies parallel to the y-axis of the image. Scale bar, 3 nm.

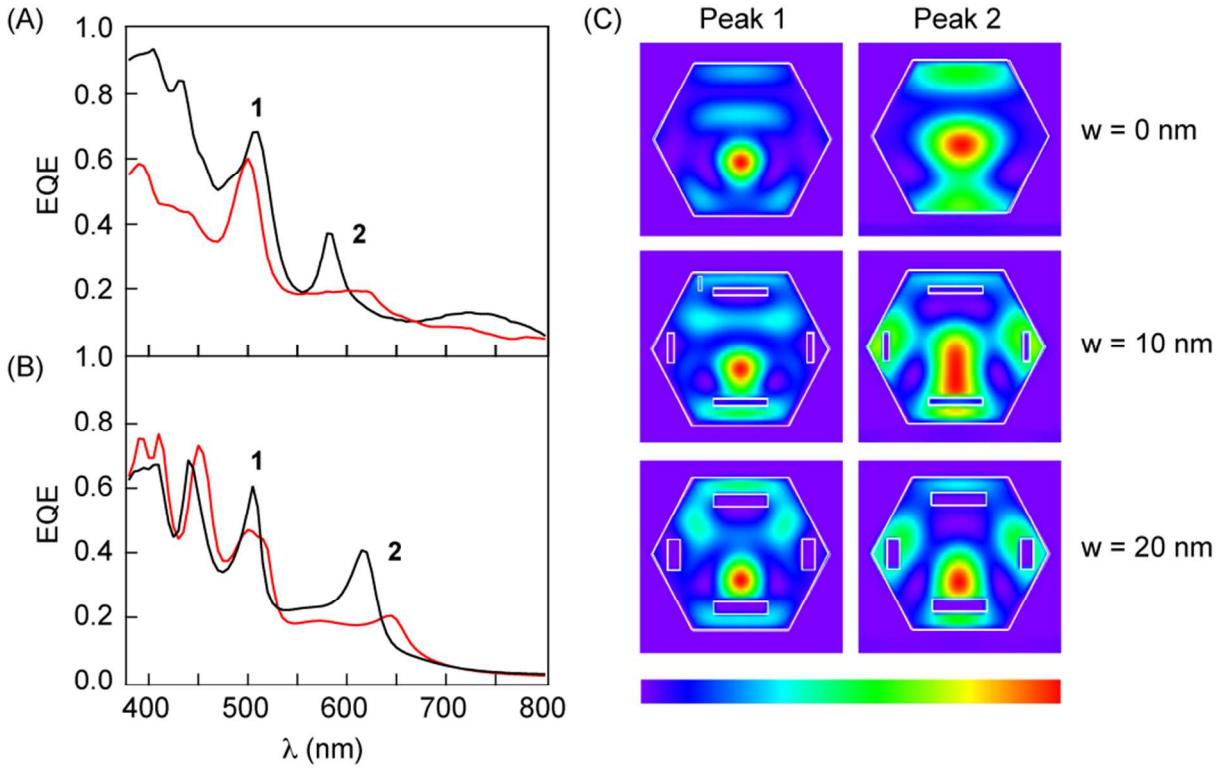

Figure S6. EQE spectra of NW devices containing nanocavities. (A) Experimental and simulated (B) absolute EQE spectra for the transverse-magnetic (TM) electric field polarization. Red and black lines correspond to nanostructures with 10 and 20 nm wide nanocavities, respectively. FDTD simulates nanostructures with hexagonal cross-sections, 230 nm diameters, and 10 and 20 nm wide cavities positioned 20 nm away from the outer Si surface of the nanostructure. SEM analyses of the devices used to obtain data in (A) show they have diameters of 224 and 236 nm. These values are within 2.6% of the simulated diameter. (C) Simulated absorption mode profiles for peak 1 (505 nm) and peak 2 (685, 645, and 615 nm) for cavity sizes of 0, 10, and 20 nm.